A DYNAMIC MODEL OF AN INNOVATIVE HIGH-TEMPERATURE SOLAR HEATING AND COOLING SYSTEM

by

Annamaria BUONOMANO, Francesco CALISE*, and Maria VICIDOMINI

Department of Industrial Engineering, University of Naples Federico II, Naples, Italy

Original scientific paper
DOI: 10.2298/TSCI151204111B

In this paper a new simulation model of a novel solar heating and cooling system based on innovative high temperature flat plate evacuated solar thermal collector is presented. The system configuration includes: flat-plate evacuated solar collectors, a double-stage LiBr-H_2O absorption chiller, gas-fired auxiliary heater, a closed loop cooling tower, pumps, heat exchangers, storage tanks, valves, mixers and controllers. The novelty of this study lies in the utilization of flat-plate stationary solar collectors, manufactured by TVP Solar, rather than concentrating ones (typically adopted for driving double-stage absorption chillers). Such devices show ultra-high thermal efficiencies, even at very high (about 200 °C) operating temperatures, thanks to the high vacuum insulation. Aim of the paper is to analyse the energy and economic feasibility of such novel technology, by including it in a prototypal solar heating and cooling system. For this purpose, the solar heating and cooling system design and performance were analysed by means of a purposely developed dynamic simulation model, implemented in TRNSYS. A suitable case study is also presented. Here, the simulated plant is conceived for the space heating and cooling and the domestic hot water production of a small building, whose energy needs are fulfilled through a real installation (settled also for experimental purposes) built up close to Naples (South Italy). Simulation results show that the investigated system is able to reach high thermal efficiencies and very good energy performance. Finally, the economic analysis shows results comparable to those achieved through similar renewable energy systems.

Key words: *solar heating and cooling, double-effect absorption chiller, dynamic energy simulation, evacuated solar thermal collectors*

Introduction

During the past few years, a significant research effort has been performed in order to promote renewable energy sources, such as: solar, wind, biomass, geothermal and hydro. In this framework, solar heating and cooling (SHC) systems are considered one of the most promising technologies, mainly during their summer operation when the cooling energy demand and the solar radiation are simultaneous [1]. As well known, solar cooling systems are mainly coupled to thermal collectors, which produce thermal energy converted in cooling energy by a thermally-driven chiller; during winter operation, the thermal energy produced by solar collectors is also used for domestic hot water (DHW), production, space heating, *etc.* [2]. The most common SHC systems are based on single-seffect H_2O-LiBr absorption chillers (ACH) characterized by higher efficiency, good commercial availability and lower capital cost. In order to achieve high conversion efficiencies, (*i. e.* the coefficient of performance,

* Corresponding author; e-mail: frcalise@unina.it

COP around 1.2) double-effect absorption chillers are used if high-temperature solar collectors are available [3]. Usually, in this case parabolic trough collectors [4-6] and compound parabolic concentrators [7, 8] are adopted. When low-medium temperature are available, single-effect absorption chillers are frequently coupled to evacuated tubes collectors [9, 10], (COP around 0.6-0.7). Several papers concerning SCH systems demonstrating that energy consumption of buildings can be potentially reduced have been investigated in literature [10-12]. A SHC system, consisting of a flat-plate solar collector array, a hot water storage tank, and an absorption chiller unit is designed and modelled in [13] to provide space heating and cooling, DHW for a building in Nicosia, Cyprus. Thermal energy produced by concentrating photovoltaic/thermal and evacuated collectors was used to provide building heating and DHW and to supply the absorption chiller [14].

In this paper, a novel design of high-temperature SHC system is proposed. In particular, the plant layout basically includes stationary non-concentrating flat-plate evacuated (10^{-9} mbar) solar collectors and a double-effect absorption chiller. Through such solar panels, several advantages can be obtained, such as:

(1) ultra-high thermal efficiency, even higher than those reached by compact concentrating devices (as an example, according to manufacturers' data − at 1,000 W per m^2, 30 °C ambient temperature and 150 °C collector temperature − the efficiency is about 60% whereas compact concentrating collectors show efficiencies around 40%),
(2) scarce performance influence to dust (there is no need to continuously clean the device, as occurs for the reflectors of concentrating collectors),
(3) scarce and cheap maintenance (similar to the one of PV systems),
(4) no need to use a solar tracking system,
(5) simple potential integration in buildings and urban areas, and
(6) no affection by defocusing issues (as can happen of concentrating devices).

The capability of such collectors was recently numerically and experimentally proven in [15]. In this study, authors presented the experimental and numerical results of a prototypal solar cooling system installed in Saudi Arabia. As a continuation of this work, this paper presents a dynamic simulation model developed (in TRNSYS) for the energy performance analysis of high-temperature SHC system. Suitable algorithms for the economic and environmental performance analysis are also included. In order to show the results achievable by the developed model, a suitable case study is presented. Some innovations are here introduced with respect to the work recently published by some of the authors [15]:

(1) system layout has been modified including a novel arrangement for the auxiliary heater,
(2) a Mediterranean weather condition is considered, and
(3) the system was re-designed in order to operate both in heating and cooling modes.

In particular, this work refers to a small non-residential building located in the weather zone of Naples (South-Italy). Here, space heating and cooling as well as DHW is supplied through the presented SHC system. At the authors' knowledge, this is the first literature paper in which all the above mentioned research findings and results are presented and discussed.

System layout

The system layout is shown in fig.1. The system includes five different loops, namely:

(1) the solar collector pressurized water (SCW), supplying heat from the flat-plate evacuated solar thermal collectors to the tank,

(2) the hot water (HW), supplying heat from the tank to the generator of the chiller (in summer) or to the heat exchanger (in winter),
(3) the cooling water (CW), providing cooling energy to the chiller,
(4) the domestic hot water (DHW), and
(5) the chilled/hot water (CHW), supplying hot (in winter) or chilled (in summer) water to the fan-coils installed in the building spaces.

In order to control the system operation, plant design includes valves, mixers and diverters.

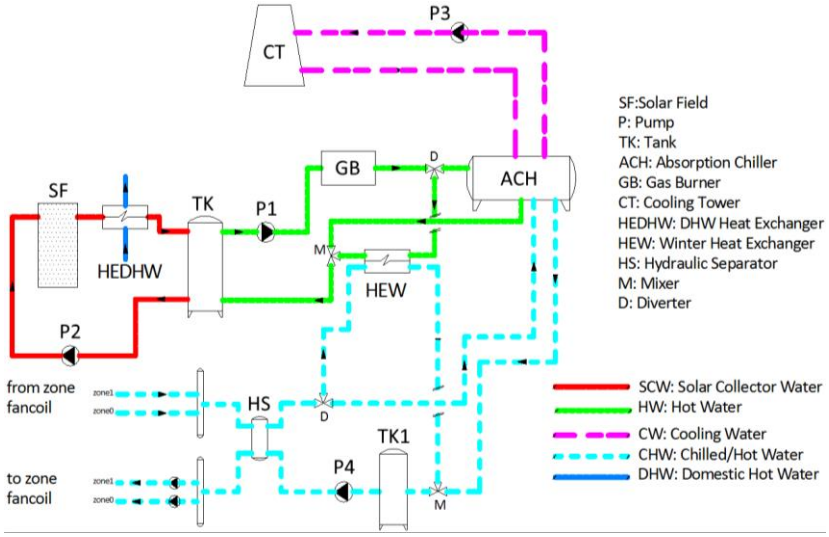

Figure 1. System layout

The system under investigation produces chilled water during summer and hot water during winter. The control strategies of the system operation are below reassumed. The solar loop, SCW, is managed by a temperature feedback controller (measuring the stratified storage tank (TK, between SCW and HW) bottom temperature, equal to the solar collector field (SF) inlet one) which varies the flow rate of variable speed pump P2 for obtaining the collectors outlet set point temperature (180 and 50 °C in summer and winter, respectively). P2 pump is started and stopped as a function of the solar radiation (*e. g.* P2 stopped if it falls below 100 W per m^2) and the SF outlet temperature (*e. g.* P2 is stopped to prevent dissipation if SF temperature is lower than TK bottom temperature), also aiming at achieving a better stability of the control system. During summer, on the load side of the TK (*i. e.* considered as stratified to reduce the number of activation/deactivations of the chiller), the HW loop fluid is pumped, by a fixed-volume pump P1, to the generator of the LiBr-H_2O double-effect absorption chiller (ACH), activated by the thermal energy provided by the solar field. Conversely, in winter, HW fluid is brought to the primary side of the plate-fin heat exchanger HEW, producing hot water for the fan-coils installed in the building. When the temperature of the fluid from P1 is lower than the fixed set-point (180 °C and 50 °C, in summer and winter respectively), an auxiliary gas-fired burner (GB) is switch on for producing hot water at fixed set-point temperature. A closed-circuit cooling tower (CT) is coupled to ACH, in order to provide cooling water (CW) to the condenser and absorber of the ACH. Hot water (HW) is used to supply heat

to the ACH which produces chilled water (CHW) to be supplied to the cooling devices, providing the possible space cooling energy demand. P3 and P4 are fixed volume pumps. P3 supplies cooled water (CW) from to cooling tower (CT) to the absorption chiller (ACH). During the summer, P4 supplies chilled water (CHW) from the absorption chiller (ACH) to the hydraulic separator (HS). Conversely, during the winter, P4 is used to bring the hot water, produced by the winter heat exchanger (HEW), to the hydraulic separator (HS). Additional secondary pumps are used to supply water to the fancoil units. The hydraulic separator (HS), required to hydraulically separate the primary and secondary loops [16], controls the mismatch between primary and secondary flows. Hot water or chilled water is supplied to the fan-coils providing the required space heating or cooling to the buildings thermal zones. Each fan-coil operates at constant air flow rate and it is equipped with a suitable thermostat operating within dead bands of ±1 °C. At last, an additional plate-fin heat exchanger (HEDHW) is also included in the solar loop. The devise, normally bypassed, is activated only when the SF outlet temperature is higher than the corresponding set point. In this case, HEDHW (acting as a heat dissipater) reduces SCF temperature down to the above mentioned set point, producing simultaneously DHW.

System model

The model of novel SHC system, presented in the previous section, designed to supply space heating and cooling and DHW to a building, is also simulated in TRNSYS environment [17]. The well-known software TRNSYS was adopted used by some of the authors in some previous studies (*e. g.* [11, 18, 19]). This section provides a brief description of the mathematical models of the solar collectors included in the simulation model. The remaining models of both built-in and user-developed components (pipes, pumps, controllers, gas-fired burner, *etc.*) are discussed in references. The models of all the components included in the systems are validated *vs*. experimental data. In particular, solar collector model was recently validated in [15], absorption chiller model is calibrated by using manufacturers' data and the models of the remaining components were taken from TRNSYS library (previously validated *vs*. real data). Finally, the TRNSYS type for building performance simulations is the Type 56 [17]. It subdivides a building into multiple zones with homogeneous properties and conditions [20]. A validation report about the whole Type 56 building model is presented in [21].

Solar collectors

The solar thermal collector has been recenlty presented by TVP Solar [22]. Such company is involved in the development of several high-performance flat-plate evacuated solar thermal collectors. For such novel devices several special patented technologies are used in order to achieve ultra-high vacuum (from 10^{-4} to 10^{-9} mbar, depending on the operating temperature) in all the operating conditions, such as:

(1) a flexible glass-metal sealing made from inorganic material to prevent the ingress of any hydrogen atoms from the surrounding area, and
(2) a getter pump that absorbs eventual entered hydrogen atoms, maintaining the vacuum throughout the service life of the collector [15, 22].

The high-vacuum is the main feature of TVP Solar collectors, which can achieve very high fluid temperatures, up to 200 °C. At 180 °C, the peak thermal power produced through the MT-Power collector is about 500 W per m^2. Therefore, due to conversion of both the beam and diffuse radiation and to the ultra-high vacuum (*i. e.* low heat losses), such efficiency is even higher than that one shown by compact parabolic concentrating solar collectors

[22]. High operating temperatures are achieved without any concentration, so that no tracking mechanism and reflectors cleaning are required, resulting in a reduction of the system capital and operating costs [22]. In order to model TVP panels, the TRNSYS Type 132 is adopted [23]. Here, the model of a flat-plate solar collector based on Hottel-Whillier equation, completed with the incidence angle modifier (IAM) coefficient, is included. In order to consider all collector designs and weather types, a set of correction terms is included. These parameters are available for all collectors tested according to ASHRAE standards [24] and to european standards [25]. This model also considered the effective thermal capacitance of the collector, wind dependencies on the zero loss efficiency and heat loss and the long-wave irradiance dependence of the heat loss. The collector efficiency is calculated as:

$$\eta = a_0 \mathrm{IAM_b} + a_0 \mathrm{IAM_d} - a_1 \frac{T_\mathrm{m} - T_\mathrm{a}}{I_\mathrm{TOT}} - a_2 \frac{(T_\mathrm{m} - T_\mathrm{a})^2}{I_\mathrm{TOT}} - a_3 u \frac{T_\mathrm{m} - T_\mathrm{a}}{I_\mathrm{TOT}} + a_4 \frac{E_\mathrm{L} - \sigma T_\mathrm{a}^4}{I_\mathrm{TOT}} - a_5 \frac{1}{I_\mathrm{TOT}} \frac{\mathrm{d}T_\mathrm{m}}{\mathrm{d}T} - a_6 u \qquad (1)$$

All the coefficients, ranging from a_1 to a_6, can be calculated by a test standard detailed in the new European test ISO 9806-3 [26]. In addition, the solar fraction was defined as the ratio between the solar energy supplied to the HEW (ACH, in summer) and the total thermal energy used by the HEW (ACH in summer).

Economic model

The presented analysis also aims at evaluating the system performance from the economic point of view. To this scope, a detailed economic model, for the calculation of both capital and operating costs (as a function of the main design and operating parameters), is implemented. For the investigated prototype, the initial capital cost, *J*, is due to the sum of solar thermal collectors cost, absorption chiller cost (including gas burner and cooling tower) and balance of the system (BOS: tank, pipes, gas burner, valves, and control system). The ACH cost is constant, being constant the building cooling demand. All other costs are assumed as a function of the components design parameters, while overall operating cost savings are calculated as the difference between the operating costs of the reference and the proposed system:

$$\Delta C_\mathrm{op} = \frac{Q_\mathrm{DHW} c_\mathrm{ng}}{\eta_\mathrm{ref} LHV_\mathrm{NG}} + \frac{Q_\mathrm{ACH,chill} c_\mathrm{EE}}{COP_\mathrm{summer,ref}} + \frac{Q_\mathrm{HEW} c_\mathrm{EE}}{COP_\mathrm{winter,ref}} - \frac{Q_\mathrm{GB} c_\mathrm{NG}}{\eta_\mathrm{GB} LHV_\mathrm{NG}} - \sum\nolimits_\mathrm{i} E_\mathrm{aux,i} c_\mathrm{EE} - C_\mathrm{M} \qquad (2)$$

The discount payback (DPB), the net present value (NPV) and the profit index (PI) are also calculated. For the DPB and NPV, a discount rate equal to 5% and a time horizon of 20 years are considered.

Case study

The system under exam is designed in order to supply space heating/cooling and DHW to a small office building located in the weather zone of Naples (South-Italy, 40°20' N-14°15' E, which features Mediterranean climate, cooling degree day = 185 Kd, heating degree day = 1,163 Kd). Weather data of Naples are obtained from the Meteonorm database. The building is a 240 m^2 two floors, including two office spaces (120 m^2 each) for each level of 3.0 m of height, and it is modelled by means of a single thermal zone per floor (zone 0 and zone 1) and a common zone including the stairs. Heating and cooling are supplied only to the office spaces (excluding the stairs – 24 m^2, which is in free floating temperature). The building glazed areas are: 9.6 of 48.0 m^2 on the East facade; 28.8 of 90 m^2 on the South fa-

cade; 9.6 of 90 m^2 on the North facade; 7.2 of 48 m^2 on the West facade. The main properties of the building elements and the model assumptions related to the operating parameters (scheduling, set point temperatures, *etc*.) are shown in tab. 1 and tab. 2, respectively. As a function of the building design, as well as on the basis of a conventional procedure for the calculation of the heating and cooling building loads [27], the main design parameters of the SHC system components are calculated, as summarized in tab. 3. Finally, the economic costs taken into account in the case study are summarized in tab. 4. The capital cost of the reference system (J_{ref}) is assumed equal to 5.0 k€. Finally, note that the Italian average energy costs are taken into account.

Table 1. Features of the modelled building envelope

Opaque elements	Thickness [cm]	U [$Wm^{-2}K^{-1}$]	M_s [kgm^{-2}]	Y_{ie} [$Wm^{-2}K^{-1}$]	Windows	U [$Wm^{-2}K^{-1}$]	g [%]	S_f [–]
Adjacent ceiling	22	1.00	310	0.23	2.00 × 1.2	2.83	0.76	0.50
External walls	30	0.87	264	0.34				
External roof	30	0.76	238	0.27				
External floor	30	0.64	238	0.82				
Internal wall	12	1.34	144	1.20				

Table 2. Operating parameters assumptions

Infiltration and air change rates [vol per h]	0.5 and 2.0
Heating and cooling seasons [–]	Nov 15th-Mar 31st and Apr 1st-Nov 14th
Heating and cooling set point temperatures [°C]	20 and 26
People sensible and latent gains [W per p]	65 and 55
People occupancy [p per m^2]	0.05
Lights and equipment gains [W per m^2]	10 and 5
Occupancy, lights and equipment gains schedules [h]	8:00-18:00 (Mon-Fri)

Table 3. Main design parameters of the modelled SHC system

Collectors area [m^2]	52.5
ACH chilled power [kW]	23
ACH nominal COP [–]	1.1
GB power [kW]	21
Tank volume (TK, TK1) [m^3]	1
Tank loss coefficient [$Wm^{-2}K^{-1}$]	0.5
Pipe length (flexible and standard) [m]	60 and 90
Pipe inside diameter (flexible and standard) [mm]	25
Pipe insulation (flexible and standard) [$Wm^{-2}K^{-1}$]	0.46 and 0.30
P1-P4, P2 and P3 rated flow rates [kg per h]	4,000, 2,000 and 7,640

Table 4. Economic parameters assumptions

Solar collector [€ per m^2]	ACH + CT + GB [k€]	BOS [€ per m^2]	J [k€]	M (maintenance) [% of J per year]	c_{EE} [€ per kWh]	c_{NG} [€ per Sm^3]
300	15.0	50	36.0	1	0.20	0.90

Results and discussion

The developed simulation tool allows one to predict the system energy performance from the energy and economic point of view. The case study office building, located in the weather zone of Naples, is dominated, as expected, by cooling demand for both zone 0 and zone 1, as shown in tab. 5. Such table reports the predicted annual energy balances of the analysed SHC system. Such results are obtained for an overall incident solar radiation, I_{TOT},

about 91 MWh per year (1.73 MWh per m^2year). Although the high collectors operating temperatures about 60 °C in winter and 180 °C in summer, their seasonal collectors' thermal efficiencies resulted to be very good, averagely equal to 63% and 32%, respectively. On the contrary, such high temperatures (especially the summer ones) imply a high magnitude of heat transfer losses in pipes and tanks. The amount of solar heat in excess is converted in DHW, Q_{HEDHW}, being a not marginal percentage, about 8.2% of the overall solar thermal production. This is due to the low storage capacity of the modelled tank (not capable to reduce the time shift between solar energy availability and space cooling demand) and to the high efficiency of the solar collectors together with the high thermal capacity of the solar field. As a result of the large solar field, very high solar fractions (0.948 and 0.967, in winter and summer, respectively) are obtained and, most of the time, HEW or ACH are only driven by solar energy, with a marginal need of the heat demanded to the GB, Q_{GB}. In fact, the space cooling demand, Q_{ACH}, chill, is 12.6 MWh per year, obtained for an average COP_{ACH} of about 1.23; whereas the space heating one, Q_{HEW}, is only 4.3 MWh per year. Concerning the economic analysis, different scenarios are taken into account. They also include possible incentives (INC), presently adopted in Italy, and the variation of the produced DHW utilization. In particular, in Italy no incentive is available for actions regarding new buildings. Conversely, in order to promote energy efficiency in existing buildings, a tax relief equal to 50% of the total investment cost is given [28]. The results of this analysis are obtained comparing the proposed system with the conventional one. In particular, the proposed renewable system was compared with the reference ones in terms of both capital and operating costs, allowing one to obtain a cash flow showing the economic performance of the proposed system. Such results are summarized in tab. 6. Here, profitable scenarios are achieved when the NPV is significantly higher than zero. In such circumstances, DPB is also significantly lower than system annuity factor FA. It also worth noting that, NPV was evaluated by taking into account the discount rate and the time horizon, by means of the factor annuity (FA). Here, in case of a high fraction (f_{DHW}) of the produced DHW, effectively used in the building, and/or in case of incentives, a very good economic profitability of the SHC system is shown.

Table 5. Yearly simulation results

	Winter/heating [kWh per y]	Summer/cooling [kWh per y]
Q_{zone}	1,485 (Zone 0) and 1,809 (Zone 1)	4,975 (Zone 0) and 7,186 (Zone 1)
Q_{sc}	12,506	22,467
Q_{HEDHW}	7,487 (59.9%)	8,223 (36.6%)
Q_{TK}	4,306	12,052
$Q_{pipeloss}$	127	697
$Q_{TK,loss}$	3,718	9,128
Q_{GB}	693	764
Q_{HEW}	4,252	–
$Q_{ACH,chill}$	–	12,591

Table 6. Economic results

	f_{DHW}		
	0	0.5	1.0
NPV [k€]	−11.9	−2.7	6.6
PI [–]	−0.51	−0.11	0.28
SPB [years]	25.4	14.1	9.7
DPB [years]	–	25.0	13.6
INC (70% of *J*) [k€]	11.7	11.7	11.7
NPV_{INC} [k€]	10.6	19.1	27.5
PI_{INC} [–]	0.9	1.6	2.4
SPB_{INC} [years]	12.7	7.1	4.9
DPB_{INC} [years]	20.7	9.0	5.8

In particular, by considering the 50% capital cost incentive (presently adopted in Italy for SHC systems), the calculated SPB vary from 4.9 to 12.7 years depending on the DHW utilization. Conversely, without any incentive, the system is economically profitable only in case of a full utilization of the produced DHW. As well known, renewable energy technologies still require some initial incentives in order to be profitable for the final user. In order to assess the

time history of the occurring system energy flows, for the hottest summer day (July 25th) and the week including it, the SHC daily and weekly operations are also discussed. In fig. 2 it is clearly shown the rapid SC outlet temperature, $T_{OUT,SC}$, observed during the early morning, reaching the set point of 180 °C. Around 11:00 a. m., $T_{OUT,SC}$ starts to increase as a consequence of the mismatch between the higher thermal capacity of the solar field and the heat demand of the ACH.

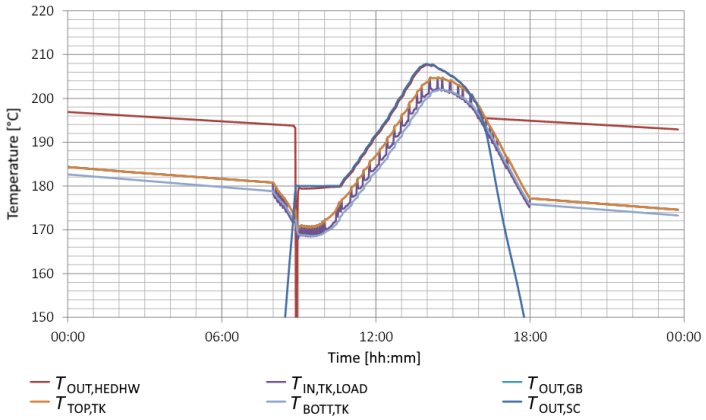

Figure 2. Temperatures – high temperature loops (July 25th)

In this day no difference is observed between SC and HEDHW outlet temperatures, *i. e.* HEDHW is never activated being $T_{OUT,SC}$ always below 210 °C. No difference is observed between TK outlet and GB outlet temperatures, *i. e.* GB is never on and the ACH is completely driven by solar energy. For the sake of completeness, fig. 3 shows the temperature oscillation of the indoor air (ranging between 24 and 26 °C) and the time history of the temperatures of the primary (P) and secondary (S) sides of the hydraulic separator (HS).

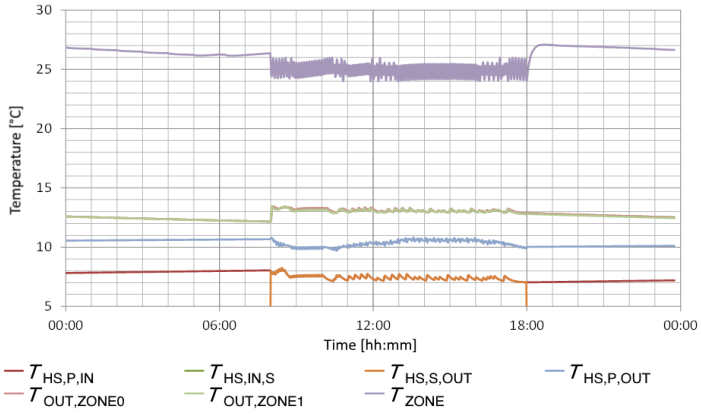

Figure 3. Temperatures – low temperature loops and zone (July 25th)

Here, it is clearly displayed that CHW supply water is stably around 7 °C, whereas the return temperature varies around 13 °C. The variation of the energy flows observed during

the year can be discussed on a weekly basis. In particular, fig. 4 shows the main energy flows of the solar loop. The variation of the heat produced by the solar field, Q_{SC}, follows the trend of the available total solar radiation (I_{TOT}, also reported in fig. 4). It is also worth noting that the distance between the two above mentioned curves (I_{TOT} and Q_{SC}) is representative of the energy loss in the solar field. Thus, such losses increase during the summer period, where the operating temperature of the solar field is much higher with respect to the winter operation (180 *vs.* 60 °C), implying a high decrease of the efficiency of the solar field. The DHW production (Q_{HEDHW}) is mainly obtained during winter, due to the much lower heat demand required for building space heating with respect to the heat demand of the absorption chiller during summer. In addition, the trend of the energy entering to and exiting from the tank TK, $Q_{TK,IN}$ and $Q_{TK,OUT}$, highlight negligible thermal losses in winter (*i. e.* the curves are basically coincident); much higher thermal losses are observed in summer due to the higher operating temperatures. Conversely, for CHW loop, the thermal losses increase in winter due to the higher temperature difference *vs.* the environment with respect to the winter case (not shown for the sake of brevity).

The heating and cooling demands (Q_{HEAT} and Q_{COOL}) of the two building zones (Zone 0 and Zone 1), and the related system energy productions are shown in fig. 5.

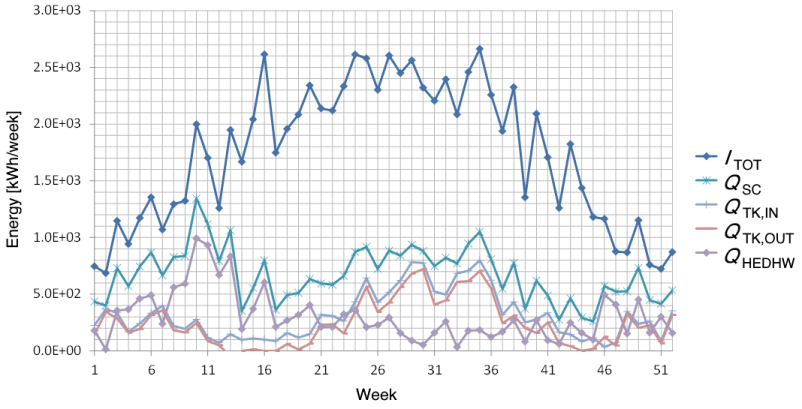

Figure 4. Weekly integrated energy, solar loop

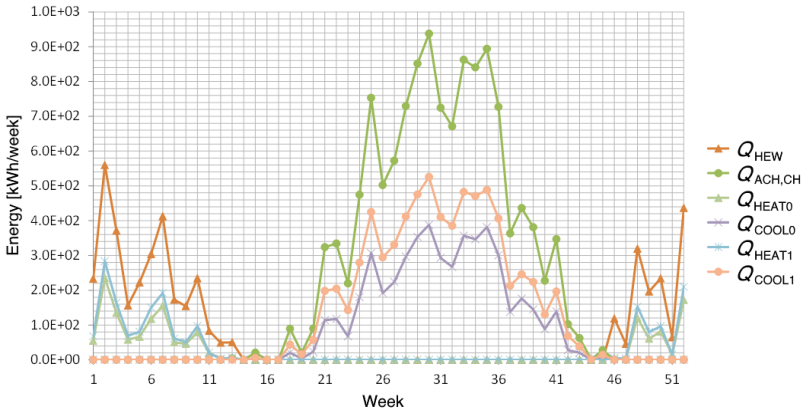

Figure 5. Weekly integrated energy, heating and cooling loops

Here, the ACH chilled production, $Q_{ACH,CH}$, reaches 950 kWh per week during the hottest summer weeks, whereas the maximum space heating demand, Q_{HEW}, is only 560 kWh per week, mainly due to the much longer cooling season with respect to the heating one. The solar loop energy performance is surprisingly high, determining a marginal amount of heat required by the gas burner. This also causes an increase of the system profitability. Thus, the SHC system investigated in this paper is particularly attractive for those applications, such as office or commercial buildings, dominated by cooling loads. Conversely, a much lower energy and economic profitability would be achieved in case of residential buildings, due to lower cooling demands. The main energy findings of this paper are summarized in fig. 6.

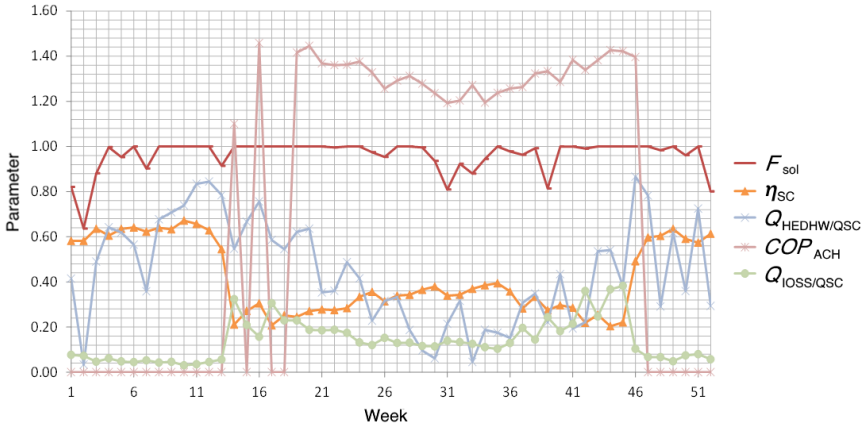

Figure 6. Weekly integrated energy, performance parameters

Here, the plotted solar fraction, F_{sol}, is regularly very high, lower results are observed during the hottest summer weeks or during the coldest winter weeks. These novel solar thermal collectors exhibit an excellent performance both in summer and in winter. In particular, during summer the efficiency ranges between 35 and 40%, besides the high system operating temperatures (180 °C). Conversely, during winter, lower temperatures (60 °C) imply a higher thermal efficiency. It is worth noting that the collector is much more sensitive to the operating temperature than to the weather conditions. At last, thermal losses become a severe issue during the summer operation, being about 20% of the total solar heat; lower losses (about 5%) are instead observed during winter.

Conclusions

This paper presents a high temperature solar heating and cooling system basically based on novel flat-plate evacuated solar thermal collectors and a double-effect absorption chiller. Additional heat is supplied by an auxiliary gas-fired heater. The system is modelled in TRNSYS in order to dynamically predict the related energy performance. A suitable case study related to an office building-SHC system built-up close to Naples, South-Italy, is developed for analysing the potentiality and the energy and economic feasibility of the novel SHC system. Simulation results show an excellent thermal efficiency of the considered solar collectors, though the high operating temperatures of the system. In fact, the efficiency of the solar collector ranges between 30% and 40%, depending on the season. This result is even

higher than the one shown by compact concentrating solar collectors. Obviously, an increase of solar collector efficiency proportionally affects the overall efficiency of the whole SHC system. In addition, a payback period lower than those achieved by similar systems is achieved. The system is very attractive in case of cooling dominated buildings and/or where a high amount of DHW is required. Concerning the developed case study, the following main results can be highlighted.

– The modelled solar field is capable to satisfy the demand of space heating and cooling and DHW for almost all the year, exhibiting ultra-high solar fractions; this is due to the high efficiency of the thermal collectors, ranging from 35 to 40% in summer (for operating temperature about 180 °C) and surpassing 60% in winter (working at lower operating temperature, around 60 °C); the system also produces a significant amount of DHW, especially in winter, increasing the system energy performance; high summer thermal losses (20% of the total solar heat) and lower winter ones (5%) are obtained, and
– The economic results show that a very good profitability of the investigated system is achieved in case of high DHW demands and/or in case of economic incentives; in particular, for the 50% capital cost incentive (adopted in Italy for SHC systems), SPB ranges from 4.9 to 12.7 years (according to the occurring DHW utilization); conversely, without incentives, the system resulted economically profitable only in case of a full utilization of the produced DHW.

Future works will be focused on the analysis of measurement data obtained through the experimental setup located in Naples, necessary to validate the developed dynamic simulation model here presented.

Nomenclature

a_1 – zero collector heat loss coefficient, [$Wm^{-2}K^{-1}$]
a_2 – temperature difference dependence of the heat loss coefficient, [$Wm^{-2}K^{-2}$]
a_3 – wind speed dependence of the heat loss coefficient, [$Jm^{-3}K^{-1}$]
a_4 – long-wave radiation dependence of the collector
a_5 – effective heat capacity of the collector, [$Jm^{-2}K^{-1}$]
a_6 – wind speed dependence in zero loss efficiency, [ms^{-1}]
C – cost, [€] or [€ per m^2]
c – unit cost, [€ per Sm^3] or [€ per kWh]
DPB – discount payback, [€]
E – wavelength radiation onto the collector plane, [Wm^{-2}]
F – solar fraction
FA – factor annuity
I – incident solar radiation, [Wm^{-2}]
NPV – net present value, [€]
PI – profit index, [–]
Q – energy, [kWh]
SPB – simple pay back, [years]
T – temperature, [°C]
u – wind speed in (parallel to) the collector plane, [ms^{-1}]

Greek symbols

η – efficiency, [–]

Subscripts

ACH – absorption chiller
a – referred to ambient
aux – auxiliaries
b – beam
CH – chilled
CT – cooling tower
d – diffuse
EE – electricity
GB – gas burner
HS – hydraulic separator
IN – inlet
L – long
M – maintenance
m – collector mean temperature
NG – natural gas
OUT – outlet
op – operating
ref – reference
SC – solar collectors
sol – solar energy
TOT – total
TK – tank

References

[1] Kalogirou, S. A., *Chapter 6 − Solar Space Heating and Cooling*, Kalogirou, S. A., (Ed.) Solar Energy Engineering (Second Edition), Academic Press, Boston, USA, 2014, pp. 323-395
[2] IEA, Current Research Projects, Task 53 − New Generation Solar Cooling and Heating Systems (PV or Solar Thermally Driven Systems)
[3] Sarbu, I., Sebarchievici, C., Review of Solar Refrigeration and Cooling Systems, *Energy and Buildings*, *67* (2013), Dec., pp. 286-297
[4] Qu, M., *et al.*, A Solar Thermal Cooling and Heating System for a Building: Experimental and Model Based Performance Analysis and Design, *Solar Energy*, *84* (2010), 2, pp. 166-182
[5] El Fadar, A., *et al.*, Modelling and Performance Study of a Continuous Adsorption Refrigeration System Driven by Parabolic trough Solar Collector, *Solar Energy*, *83* (2009), 6, pp. 850-861
[6] Calise, F., High Temperature Solar Heating and Cooling Systems for Different Mediterranean Climates: Dynamic Simulation and Economic Assessment, *Applied Thermal Eng.*, *32* (2012), Jan., pp. 108-124
[7] Hang, Y., *et al.*, Experimental Based Energy Performance Analysis and Life Cycle Assessment for Solar Absorption Cooling System at University of Californian, Merced, *Energy and Buildings, 82* (2014), Oct., pp. 746-757
[8] Zeyu, L., *et al.*, Performance Analysis of Solar Air Cooled Double Effect LiBr/H_2O Absorption Cooling System in Subtropical City, *Energy Conversion and Management, 85* (2014), Sep., pp. 302-312
[9] Hang, Y., *et al.*, Economical and Environmental Assessment of an Optimized Solar Cooling System for a Medium-sized Benchmark Office Building in Los Angeles, California, *Renewable Energy, 36* (2011), 2, pp. 648-658
[10] Buonomano, A., *et al.*, Solar Heating and Cooling Systems by CPVT and ET Solar Collectors: A Novel Transient Simulation Model, *Applied Energy, 103* (2013), Mar., pp. 588-606
[11] Buonomano, A., *et al.*, Thermoeconomic Analysis of Storage Systems for Solar Heating and Cooling Systems: A Comparison between Variable-volume and Fixed-volume Tanks, *Energy*, *59* (2013), Sep., pp. 600-616
[12] Xu, D., *et al.*, Multi-objective Optimal Design of a Solar Absorption Cooling and Heating System under Life-cycle Uncertainties, *Sustainable Energy Technologies and Assessments*, *11* (2015), Sep., pp. 92-105
[13] Arsalis, A., Alexandrou, A. N., Parametric Study and Cost Analysis of a Solar-heating-and-cooling System for Detached Single-family Households in Hot Climates, *Solar Energy*, *117* (2015), July, pp. 59-73
[14] Sanaye, S., Sarrafi, A., Optimization of Combined Cooling, Heating and Power Generation by a Solar System, *Renewable Energy*, *80* (2015), July, pp. 699-712
[15] Buonomano, A., *et al.*, Experimental Analysis and Dynamic Simulation of a Novel High-temperature Solar Cooling System, *Energy Conversion and Management*, *109* (2016), Feb., pp. 19-39
[16] Calise, F., Thermoeconomic Analysis and Optimization of High Efficiency Solar Heating and Cooling Systems for Different Italian School Buildings and Climates, *Energy and Buildings*, *42* (2010), 7, pp. 992-1003
[17] Klein, S. A., Solar Energy Laboratory, TRNSYS, University of Wisconsin, Madison, A Transient System Simulation Program, 2006
[18] Calise, F., High Temperature Solar Heating and Cooling Systems for Different Mediterranean Climates: Dynamic Simulation and Economic Assessment, *Applied Thermal Eng.*, *32* (2012), 1, pp. 108-124
[19] Calise, F., *et al.*, Design and Parametric Optimization of an Organic Rankine Cycle Powered by Solar Energy, *Americal Journal of Engineering and Applied Science*, *6* (2013), 2, pp. 178-204
[20] Buonomano, A., *et al.*, Dynamic Energy Performance Analysis: Case Study for Energy Efficiency Retrofits of Hospital Buildings, *Energy*, *78* (2014), Dec., pp. 555-572
[21] Voit, P., *et al.*, Common EC Validation Procedure for Dynamic Building Simulation Programs – Application with TRNSYS, TRANSSOLAR GmbH – Conference of International Simulation Societies – Zürich
[22] Nishioka, K., *et al.*, Annual Output Estimation of Concentrator Photovoltaic Systems Using High-efficiency InGaP/InGaAs/Ge Triple-junction Solar Cells Based on Experimental Solar Cell's Characteristics and Field-test Meteorological Data, *Solar Energy Materials and Solar Cells*, *90* (2006), 1, pp. 57-67
[23] Bengt, P., Bales, C., Report of IEA SHC − Task 26, Solar Combisystems, 2002

[24] ***, American Society of Heating, Refrigerating and Air-Conditioning Engineers, 2003 Ashrae Handbook: Heating, Ventilating, and Air-Conditioning Applications, ASHRAE, 2003
[25] Lazzaretto, A., Tsatsaronis, G., SPECO: A Systematic and General Methodology for Calculating Efficiencies and Costs in Thermal Systems, *Energy*, *31* (2006), 8-9, pp. 1257-1289
[26] ***, ISO, 9806-3, Thermal Performance of Unglazed Liquid Heating Collectors, 1995
[27] Kreider, J. F., *et al.*, *Heating and Cooling of Buildings: Design for Efficiency*, CRC Press, Boca Raton, Fla., USA, 2010
[28] ***, 3 Agosto 2013, n. 90, Art. 14 "Tax Relief for Energy Efficiency Measures" (European Directive, 2010/31/UE)

Paper submitted: December 4, 2015
Paper revised: January 29, 2016
Paper accepted: April 5, 2016